

Exotic quantum spin models in spin-orbit-coupled Mott insulators

J. Radić,¹ A. Di Ciolo,^{1,2} K. Sun,^{1,3} and V. Galitski^{1,3}

¹*Joint Quantum Institute and Department of Physics,
University of Maryland, College Park, Maryland 20742-4111, USA*

²*Department of Physics, Georgetown University, Washington, D.C. 20057, USA*

³*Condensed Matter Theory Center, Physics Department,
University of Maryland, College Park, Maryland 20742-4111, USA*

(Dated: March 3, 2013)

We study cold atoms in an optical lattice with synthetic spin-orbit coupling in the Mott-insulator regime. We calculate the parameters of the corresponding tight-binding model using Peierls substitution and “localized Wannier states method” and derive the low-energy spin Hamiltonian for fermions and bosons. The spin Hamiltonian is a combination of Heisenberg model, quantum compass model and Dzyaloshinskii-Moriya interactions and it has a rich classical phase diagram with collinear, spiral and vortex phases.

PACS numbers:

Since the first experimental realization of Bose-Einstein condensate (BEC), cold atoms have proven to be an excellent playground for studying many-body physics [1, 2] and many interesting phenomena take place for strongly interacting atoms in an optical lattice. These studies started with an experimental observation of superfluid to Mott-insulator phase transition [3] which was followed by experimental and theoretical work on both Bose and Fermi gases in lattices of different dimensionality and in various parameter regimes [1, 2]. The key features of cold atoms in optical lattices are the excellent tunability of parameters and the fact that the sample is almost perfectly described by the Hubbard model in the deep lattice regime [2]. Since it is well known that the Hubbard model is mapped to an effective spin Hamiltonian for Mott-insulator phases with integer filling [4], it is clear that cold atoms can be used to “engineer” various quantum spin systems [5, 6] from those described by the Heisenberg model to more exotic ones, like the Kitaev model [7]. In designing effective spin systems different tools like polar molecules [8] and tilted optical lattices [9] can also be used. In recent years there has been a lot of interest in creating artificial Abelian and non-Abelian gauge fields in cold-atom systems [10] and successful experimental realizations of synthetic magnetic [11, 12] and electric field [13] and spin-orbit coupling (SOC) [14] have been reported. The role of SOC in cold atoms has been extensively studied following the theoretical proposal for the creation of artificial SOC [15, 16] and rich phase diagrams have been found in BECs [17–19] and fermionic systems [20–22].

In this letter we combine optical lattice and SOC which, in the deep lattice regime, leads to tight-binding description with non-zero “spin-flip” hopping between neighboring sites [23]. We show that in the Mott-insulator phase with integer filling the system is described by an interesting effective spin Hamiltonian which is a combination of Heisenberg model, quantum

compass model and Dzyaloshinskii-Moriya terms. We note that combination of an optical lattice and SOC has already been considered with a purpose of studying superfluid-insulator transition [24], topological phase transitions [25] and BEC dynamics [26]. In the context of solid-state physics spin models resulting from Mott-insulators with strong SOC were studied in Ref. [27–30].

We study a two-dimensional system of pseudospin-1/2 atoms on a square optical lattice with synthetic SOC. The single-particle physics is described by the Hamiltonian:

$$H_0 = \left[\frac{\mathbf{p}^2}{2m} + V_x \sin^2(Kx) + V_y \sin^2(Ky) \right] \hat{\mathbf{I}} + \alpha \tilde{\sigma}_x p_x + \beta \tilde{\sigma}_y p_y, \quad (1)$$

with \mathbf{p} and m being the atomic momentum and mass; V_x, V_y the lattice depth in x and y direction, $K = \pi/a$ (a is the lattice spacing), $\hat{\mathbf{I}}$ the 2×2 unit matrix, $\tilde{\sigma}_i$ Pauli matrices; α and β characterize the SOC. Since (1) is invariant under lattice translations, its eigenstates have Bloch-wave form: $\vec{\psi}_{\mathbf{k},n}(\mathbf{r}) = \exp(i\mathbf{k} \cdot \mathbf{r}) \vec{u}_{\mathbf{k},n}(\mathbf{r})$ and $\vec{u}_{\mathbf{k},n}(\mathbf{r} + \mathbf{R}) = \vec{u}_{\mathbf{k},n}(\mathbf{r})$, \mathbf{R} being a lattice vector. We are interested in the deep lattice regime in which pairs of energy bands are well separated and the low-energy physics is captured by the lowest pair of bands which touch at $\mathbf{k} = (0, 0)$, $(0, K)$, $(K, 0)$ and (K, K) in the energy spectrum. In this regime the system is well described by the tight-binding approximation in which the Hilbert space is spanned by states localized on individual lattice sites and the tunneling exists only between nearest-neighbor sites. There are two localized states per site ($|W_{\mathbf{R}}^1\rangle, |W_{\mathbf{R}}^2\rangle$), hence we have two effective particle species. This is the most general tight-binding description of (1):

$$H_T = - \sum_{\mathbf{r}, j} \sum_{\gamma=x,y} [a_{\mathbf{r},i}^\dagger T_\gamma^{(i,j)} a_{\mathbf{r}+\boldsymbol{\eta}_{\gamma,j}} + \text{H.c.}], \quad (2)$$

where $a_{\mathbf{r},i}^\dagger$ ($a_{\mathbf{r},i}$) creates (annihilates) a particle in the

state $|W_{\mathbf{r}}^i\rangle$, $T_{\gamma}^{(i,j)} = -\langle W_{\mathbf{r}}^i | H_0 | W_{\mathbf{r}+\boldsymbol{\eta}_{\gamma}}^j \rangle$ are the tunneling matrices and $\boldsymbol{\eta}_{\gamma} = a\hat{\gamma}$. In finding the elements of T_{γ} corresponding to H_0 , we use Peierls substitution and “localized Wannier states (LWS) method”. We write SOC in a gauge-field form: $\mathbf{p}^2/(2m) + \alpha\tilde{\sigma}_x p_x + \beta\tilde{\sigma}_y p_y = (\mathbf{p} - \mathbf{A})^2/(2m) + \text{const.}$ with $\mathbf{A} = (-m\alpha\tilde{\sigma}_x, -m\beta\tilde{\sigma}_y)$ and may use Peierls substitution to find tunneling matrices

$$T_{\gamma} = t_{\gamma} e^{-iaA_{\gamma}} = t_{\gamma} e^{i\theta_{\gamma}\tilde{\sigma}_{\gamma}}, \quad \gamma = x, y \quad (3)$$

where t_{γ} are tunneling coefficients in the γ -direction in the absence of SOC, $\theta_x = \pi\alpha'/2$, $\theta_y = \pi\beta'/2$; α' and β' are dimensionless SOC strengths: $\alpha' = 2m\alpha/(\hbar K)$, $\beta' = 2m\beta/(\hbar K)$. However, Peierls substitution is only an approximation, valid for SOC weak with respect to the kinetic plus lattice part of H_0 . This is the case when $\alpha' \ll 2\sqrt{V_x/E_R}$, $\beta' \ll 2\sqrt{V_y/E_R}$, where $E_R = \hbar^2 K^2/(2m)$ is the lattice recoil energy. While the SOC is quite weak in solid-state systems, in cold-atom systems it is typically very strong and in that case Peierls substitution is not completely valid. For example, if we combine optical lattice with spacing $a = 410$ nm and Rashba SOC generated by a scheme described in Ref. [31], we obtain $\alpha' \approx 1$, while the usual experimental values of lattice depth are $\sqrt{V_{x,y}/E_R} \sim 2 - 5$ (for smaller values of $V_{x,y}$ the tight-binding approximation is not valid). For the SOC scheme experimentally realized [14] $\alpha' \approx 1.4$. Since the validity condition for Peierls substitution is not completely satisfied, we calculate tunneling matrices using LWS method which is more involved and requires numerical approach but it does not contain any approximation. In a system with $N_x N_y$ sites and periodic boundary conditions, Wannier states for a single band are defined as [32, 33]: $|W_{\mathbf{r}}\rangle = \frac{1}{\sqrt{N_x N_y}} \sum_{\mathbf{k}} e^{-i\mathbf{k}\cdot\mathbf{r}} e^{i\varphi(\mathbf{k})} |\psi_{\mathbf{k}}\rangle$, where $|\psi_{\mathbf{k}}\rangle$ are Bloch states and $\varphi(\mathbf{k})$ is an arbitrary phase. In the absence of SOC it is possible to obtain maximally LWS by varying the phase $\varphi(\mathbf{k})$ of each Bloch state $|\psi_{\mathbf{k}}\rangle$ [33] and in the deep lattice regime these maximally LWS are well localized on individual sites. In the presence of SOC it is generally not possible to have Wannier states localized on individual sites if these are constructed from Bloch states of a single band. Therefore we consider generalized Wannier states introduced in Ref. [34]: $|W_{\mathbf{r}}^m\rangle = \frac{1}{\sqrt{N_x N_y}} \sum_{\mathbf{k}, n} e^{-i\mathbf{k}\cdot\mathbf{r}} M_{mn}(\mathbf{k}) |\psi_{\mathbf{k}, n}\rangle$, where $M_{mn}(\mathbf{k})$ are 2×2 unitary matrices which mix Bloch states of the two bands. We find maximally LWS by minimizing the functional $\Omega = \sum_{n=1}^2 [\langle r^2 \rangle_n - \langle \mathbf{r} \rangle_n^2]$ with respect to matrix elements of $M_{mn}(\mathbf{k})$ ($\langle \dots \rangle_n$ is an expectation value associated to $|W_{\mathbf{r}}^n\rangle$). The minimization is done numerically and example of an algorithm is given in Ref. [34]. Numerical results show that the tunneling matrices still have the form given in (3) but now the parameters t_x , t_y , θ_x and θ_y are some more general functions of V_x , V_y , α , β , K and m . It can be shown that the structure of tunneling matrices (3) follows from the symmetries of H_0 .

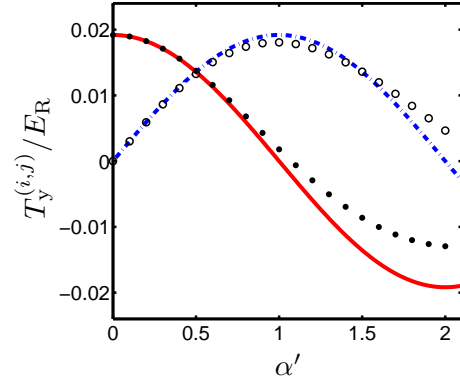


FIG. 1: (color online) Tunneling amplitudes $T_y^{(1,1)}$ and $T_y^{(1,2)}$ obtained by Peierls substitution (full red and dash-dotted blue line) and localized Wannier states method (full dots and empty circles) for different strengths of Rashba SOC and $V_x = V_y = 10 E_R$.

Peierls substitution has the advantage to give an analytical form for tunneling matrices, however it does not give any information about the Wannier states, whereas the LWS method explicitly gives states $|W_{\mathbf{r}}^1\rangle$, $|W_{\mathbf{r}}^2\rangle$ which is important in interpreting the experimental data. In Fig. 1 we compare tunneling amplitudes in the Rashba-coupling case obtained by Peierls substitution and LWS method for $V_x = V_y = 10 E_R$. They show excellent accord for small α' and sizable differences for larger ones.

Cold atoms in optical lattices are described by the tunneling Hamiltonian (2) plus interactions [2]:

$$V = \frac{1}{2} \sum_{\mathbf{r}, i, j} U_{ij} : n_{\mathbf{r}, i} n_{\mathbf{r}, j} : , \quad (4)$$

where $n_{\mathbf{r}, i}$ is a number of particles in state $|W_{\mathbf{r}}^i\rangle$, U_{ij} are interaction coefficients and $:(...):$ denotes normal ordering of creation and annihilation operators.

We are interested in the Mott-insulator regime with $t_x/U_{ij} \ll 1$, $t_y/U_{ij} \ll 1$ and integer number ν of atoms per site ($\nu = 1$ for fermions and any integer ν for bosons). In this case interactions (4) are the dominant part in the full Hamiltonian $H = H_T + V$ and we may treat the problem perturbatively by taking V as starting Hamiltonian and H_T as perturbation. The ground state of V is a state with uniform distribution of atoms and the ground state degeneracy is very large since there are two states per site that atoms can occupy. The perturbation H_T couples the ground-state manifold and excited states of V and the resulting low-energy effective Hamiltonian can be calculated in the second order of perturbation theory [5, 6]:

$$(H_{\text{eff}})_{\alpha\beta} = - \sum_{\gamma} \frac{(H_T)_{\alpha\gamma} (H_T)_{\gamma\beta}}{E_{\gamma} - (E_{\alpha} + E_{\beta})/2}, \quad (5)$$

where α and β label states in the ground-state manifold, while γ labels the excited states of V .

We first calculate the effective low-energy Hamiltonian for fermions. Since two fermions cannot occupy the same quantum state the only interesting regime is when $\nu = 1$. The only relevant interaction coefficient is $U_{12} = U$ and the excited states of V are those with two fermions of different species at the same site. Now it is convenient to introduce isospin operators: $S_{\mathbf{r}}^x = (a_{\mathbf{r},1}^\dagger a_{\mathbf{r},2} + a_{\mathbf{r},2}^\dagger a_{\mathbf{r},1})/2$, $S_{\mathbf{r}}^y = -i(a_{\mathbf{r},1}^\dagger a_{\mathbf{r},2} - a_{\mathbf{r},2}^\dagger a_{\mathbf{r},1})/2$ and $S_{\mathbf{r}}^z = (n_{\mathbf{r},1} - n_{\mathbf{r},2})/2$. Using (5) we obtain

$$H_F = \sum_{\mathbf{r}' - \mathbf{r} = \boldsymbol{\eta}_x} \left[J_h^x \mathbf{S}_{\mathbf{r}} \cdot \mathbf{S}_{\mathbf{r}'} + J_{\text{cm}}^x S_{\mathbf{r}}^x S_{\mathbf{r}'}^x + \mathbf{D}^x \cdot (\mathbf{S}_{\mathbf{r}} \times \mathbf{S}_{\mathbf{r}'}) \right] + \sum_{\mathbf{r}' - \mathbf{r} = \boldsymbol{\eta}_y} \left[J_h^y \mathbf{S}_{\mathbf{r}} \cdot \mathbf{S}_{\mathbf{r}'} + J_{\text{cm}}^y S_{\mathbf{r}}^y S_{\mathbf{r}'}^y + \mathbf{D}^y \cdot (\mathbf{S}_{\mathbf{r}} \times \mathbf{S}_{\mathbf{r}'}) \right], \quad (6)$$

where $J_h^i = J_i \cos(2\theta_i)$, $J_{\text{cm}}^i = 2J_i \sin^2 \theta_i$, $\mathbf{D}^x = J_x \sin(2\theta_x) \hat{x}$, $\mathbf{D}^y = J_y \sin(2\theta_y) \hat{y}$, $J_i = 4t_i^2/U$ and θ_i are introduced in (3). The Hamiltonian is a combination of Heisenberg model, compass model and Dzyaloshinskii-Moriya-type terms; for $\theta_x = \theta_y = 0$ (no SOC) and $J_x = J_y$ we recover the Heisenberg model [4–6].

Next we find the effective low-energy Hamiltonian for bosons, and now the number of atoms per site ν can be greater than one. The calculation for any ν and general interaction coefficients is very cumbersome, however it simplifies for $\delta U_{mn} \ll U$, where $U_{mn} = U + \delta U_{mn}$ or when $\nu = 1$ [5]. We express the Hamiltonian in terms of spin- $\nu/2$ operators defined in the same way as in the previous case. For $\delta U_{mn} \ll U$, the Hamiltonian in the first order of $\delta U/U$ is $H_{\nu B} = -H_F + \sum_{\mathbf{r}} [A(S_{\mathbf{r}}^z)^2 - h_{\nu} S_{\mathbf{r}}^z]$ where $A = (U_{11} + U_{22} - 2U_{12})/2$ and $h_{\nu} = -(\nu - 1)(U_{11} - U_{22})/2$.

For $\nu = 1$ and general U_{mn} we obtain

$$H_{1B} = - \sum_{i=x,y} \sum_{\mathbf{r}' - \mathbf{r} = \boldsymbol{\eta}_i} \left[J_h^i \mathbf{S}_{\mathbf{r}} \cdot \mathbf{S}_{\mathbf{r}'} + J_{\text{cm}}^i S_{\mathbf{r}}^i S_{\mathbf{r}'}^i + J_z^i S_{\mathbf{r}}^z S_{\mathbf{r}'}^z + \mathbf{D}_B^i \cdot (\mathbf{S}_{\mathbf{r}} \times \mathbf{S}_{\mathbf{r}'}) \right] - h_1 \sum_{\mathbf{r}} S_{\mathbf{r}}^z \quad (7)$$

where $J_z^i = (u_1 + u_2 - 2)J_h^i$, $J_{\text{cm}}^i = 2J_i \sin^2 \theta_i$, $\mathbf{D}_B^i = (u_1 + u_2)\mathbf{D}^i/2$, $h_1 = (u_1 - u_2)(J_x \cos^2 \theta_x + J_y \cos^2 \theta_y)$, $u_1 = U_{12}/U_{11}$, $u_2 = U_{12}/U_{22}$ and J_x, J_y are given in (6) with U replaced by U_{12} . Since the atoms usually used in experiments have almost spin-independent interactions we assume $U_{ij} = U$ ($u_1 = u_2 = 1$): this simplifies the Hamiltonian and yields $H_{1B} = -H_F$.

We intend to find the classical zero-temperature phase diagram of (7) with $u_1 = u_2 = 1$. Some previous papers presented models combining Heisenberg, Dzyaloshinskii-Moriya and compass-model interactions [27–29] but they did not provide a complete phase diagram, neither at a classical level, usually considering only small SOC. In our approach we treat the spins \mathbf{S}_i as classical vectors and we

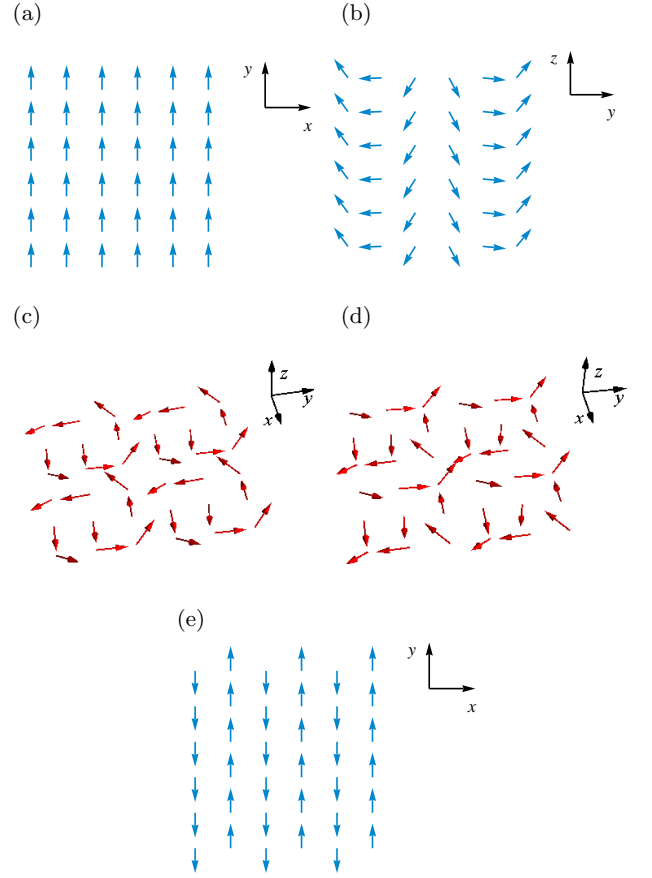


FIG. 2: (color online) Spin textures: (a) ferromagnet ($\theta_x = \theta_y = 0$); (b) spiral wave ($\theta_x = 0.5$, $\theta_y = 0.2$); (c) vortex phase ($\theta_x = \theta_y = 1$); (d) antivortex phase ($\theta_x = 2.14$, $\theta_y = 0.96$); (e) stripes ($\theta_x = 1.6$, $\theta_y = 0.7$). Phases (a), (b) and (e) are coplanar and shown in a two-dimensional representation.

aim to find the configurations $\{\mathbf{S}_i\}$ which minimize the energy, with constant $J_x = J_y$. We did our computations usually on 60×60 -site lattices and finite-size effects are negligible. In Fig. 2 we show the phases and in Fig. 3 the corresponding phase diagram. We obtain two Ising-type phases [ferromagnet (Fig. 2a) and stripes (Fig. 2e)], coplanar spirals (Fig. 2b) and three-dimensional ordered phases with vortices (Fig. 2c) or antivortices (Fig. 2d). In describing our results, it is helpful to focus on a so called “basic region” given by the triangle $\theta_y \leq \theta_x \leq \pi/2$: the solutions for other parameters can be obtained by simple mappings, e.g. ground-state configurations in $\theta_x \leq \theta_y \leq \pi/2$ region are obtained by simultaneous $\pi/2$ -rotation of spins and sites of ground states in the “basic region”. Upon activating SOC, the ferromagnet is immediately replaced by spiral waves, whose spatial periodicity reduces from several to three sites upon increasing θ_x and θ_y ; we found both commensurate and incommensurate waves. When the compass-model term becomes dominant over the Dzyaloshinskii-Moriya one, another coplanar phase appears, the ferromagnetic stripe order, either

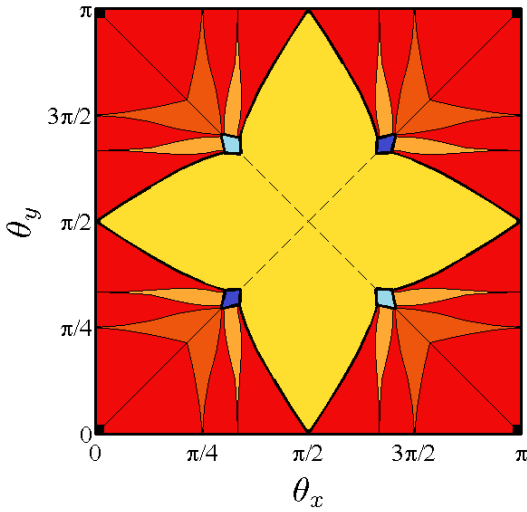


FIG. 3: (color online) Classical phase diagram of the Hamiltonian H_{1B} (see text for details): ferromagnet (black corner dots); spiral waves [dark orange (commensurate with four-sites periodicity), light orange (commensurate with three-sites periodicity), red (others)]; stripes (yellow); vortex phase (dark blue) and antivortex phase (light blue).

directly or via the three-dimensional ordered phases. We always find non degenerate classical ground states, except along the dashed lines (Fig. 3) which indicate points in the parameter space with a continuous degeneracy of classical ground states. However, we expect this degeneracy to be removed by slight deviations of the realistic engineered SOC with respect to the Rashba-Dresselhaus form of the coupling [31]. The dashed lines also represent the boundaries between phases with stripes of different orientation, *i.e.* between the phase shown in Fig. 2e and the one obtained by rotating the sites and spins of the latter by $\pi/2$ around the z -axis. The vortex phase (Fig. 2c) takes place along the diagonal $\theta_x = \theta_y$: vortices are left-handed in the region with smaller SOC and right-handed in the one with larger SOC. The antivortex phase (Fig. 2d) is found along the diagonal $\theta_y = \pi - \theta_x$ and the configuration (d) is obtained from the phase (c) by a transformation which reflects sites (but not spins) with respect to the x -axis. For a better identification of the phase properties, we consider their behavior with respect to the breaking of the translational symmetry of (7). While all the phases (except the ferromagnet) break this symmetry, they do it in a different way, *i.e.* the stripe phase in Fig. 2e is not invariant under one-lattice-site translation along x -direction, but it is invariant under two-lattice-sites translations in x -direction and under one-lattice-site translation in y -direction; the phases with vortices or antivortices are not invariant under one- and two-lattice-sites translations in x and y -direction, but they are invariant under three-lattice-sites translations. Then we can understand the evolution from stripe to vortex phase as a transition in which two-lattice-sites

translational symmetry becomes broken. The same reasoning applies for the rest of the phase diagram.

It is important to emphasize that the classical analysis yields no gapless modes in the whole parameter region except for the diagonal lines ($\theta_y = \theta_x$, $\theta_y = \pi - \theta_x$) in the stripe region. The absence of these gapless modes provides stronger guidelines for further analysis in a semiclassical or quantum approach.

In summary, we studied the effects of spin-orbit coupling in cold atoms in an optical lattice in the Mott-insulating regime. We derived the tight-binding model using Peierls substitution and Localized Wannier State method and obtained the effective low-energy Hamiltonian for fermions and bosons: this takes the form of an exotic spin model with Heisenberg, compass-model and Dzyaloshinskii-Moriya interactions. We determined the classical phase diagram for this model and showed that the interplay between the different interactions is responsible for a large variety of phases: ferromagnet, spirals, stripes, three-dimensional vortex and antivortex phases. We expect that our classification of ground states could generally survive in a quantum approach; in fact, except for some particular cases we mentioned in the discussion, on the classical level there are no degeneracies which would be lifted by quantum fluctuations.

We thank W.S. Cole, S. Zhang, A. Paramekanti and N. Trivedi for discussions. J.R. thanks Stephen Powell and Qinqin Lu for discussions. This research was supported by US-ARO, JQI (A.D.C. and V.G.), ARO-MURI (J.R.) and JQI-NSF-PFC (K.S.).

-
- [1] M. Lewenstein, A. Sanpera, V. Ahufinger, B. Damski, A. S. De, and U. Sen, *Adv. Phys.* **56**, 243 (2007).
 - [2] I. Bloch, J. Dalibard, and W. Zwerger, *Rev. Mod. Phys.* **80**, 885 (2008).
 - [3] M. Greiner, M. O. Mandel, T. Esslinger, T. Hänsch, and I. Bloch, *Nature* **415**, 39 (2002).
 - [4] A. H. MacDonald, S. M. Girvin, and D. Yoshioka, *Phys. Rev. B* **37**, 9753 (1988).
 - [5] A. B. Kuklov and B. V. Svistunov, *Phys. Rev. Lett.* **90**, 100401 (2003).
 - [6] L.-M. Duan, E. Demler, and M. D. Lukin, *Phys. Rev. Lett.* **91**, 090402 (2003).
 - [7] A. Y. Kitaev, *Ann. Phys.* **321**, 2 (2006).
 - [8] A. Micheli, G. K. Brennen, and P. Zoller, *Nat. Phys.* **2**, 341 (2006).
 - [9] J. Simon, W. S. Bakr, R. Ma, M. E. Tai, P. M. Preiss, and M. Greiner, *Nature* **472**, 307 (2011).
 - [10] J. Dalibard, F. Gerbier, G. Juzeliūnas, and P. Öhberg, *Rev. Mod. Phys.* **83**, 1523 (2011).
 - [11] Y.-J. Lin, R. L. Compton, K. Jimenez-Garcia, J. V. Porto, and I. B. Spielman, *Nature* **462**, 628-632 (2009).
 - [12] M. Aidelsburger, M. Atala, S. Nascimbene, S. Trotzky, Y.-A. Chen, and I. Bloch, *Phys. Rev. Lett.* **107**, 255301 (2011).
 - [13] Y.-J. Lin, R. L. Compton, K. Jimenez-Garcia, W. D.

- Phillips, J. V. Porto, and I. B. Spielman, *Nature Physics* **7**, 531-534 (2011).
- [14] Y.-J. Lin, K. Jimenez-Garcia, and I. B. Spielman, *Nature* **471**, 83-86 (2011).
 - [15] T. D. Stanescu, C. Zhang, and V. M. Galitski, *Phys. Rev. Lett.* **99**, 110403 (2007).
 - [16] J. Ruseckas, G. Juzeliūnas, P. Öhberg, and M. Fleischhauer, *Phys. Rev. Lett.* **95**, 010404 (2005).
 - [17] T. D. Stanescu, B. Anderson, and V. Galitski, *Phys. Rev. A* **78**, 023616 (2008).
 - [18] C. Wang, C. Gao, C.-M. Jian, and H. Zhai, *Phys. Rev. Lett.* **105**, 160403 (2010).
 - [19] S. Sinha, R. Nath, and L. Santos, *Phys. Rev. Lett.* **107**, 270401 (2011).
 - [20] M. Sato, Y. Takahashi, and S. Fujimoto, *Phys. Rev. Lett.* **103**, 020401 (2009).
 - [21] M. Iskin and A. L. Subasi, *Phys. Rev. A* **84**, 043621 (2011).
 - [22] S. Takei, C.-H. Lin, B. M. Anderson, and V. Galitski, *Phys. Rev. A* **85**, 023626 (2012).
 - [23] N. Goldman, A. Kubasiak, A. Bermudez, P. Gaspard, M. Lewenstein, and M. A. Martin-Delgado, *Phys. Rev. Lett.* **103**, 035301 (2009).
 - [24] T. Graß, K. Saha, K. Sengupta, and M. Lewenstein, *Phys. Rev. A* **84**, 053632 (2011).
 - [25] N. Goldman, W. Buegeling, and C. M. Smith, *Europhys. Lett.* **97**, 23003 (2012).
 - [26] J. Larson, J.-P. Martikainen, A. Collin, and E. Sjöqvist, *Phys. Rev. A* **82**, 043620 (2010).
 - [27] L. Stekhtman, O. Entin-Wohlman, and A. Aharony, *Phys. Rev. Lett.* **69**, 836 (1992).
 - [28] L. Stekhtman, O. Entin-Wohlman, and A. Aharony, *Phys. Rev. B* **47**, 174 (1993).
 - [29] A. Zheludev, S. Maslov, G. Shirane, I. Tsukada, T. Masuda, K. Uchinokura, I. Zaliznyak, R. Erwin, and L. P. Regnault, *Phys. Rev. B* **59**, 11432 (1999).
 - [30] G. Jackeli and G. Khaliullin, *Phys. Rev. Lett.* **102**, 017205 (2009).
 - [31] D. L. Campbell, G. Juzeliūnas, and I. B. Spielman, *Phys. Rev. A* **84**, 025602 (2011).
 - [32] G. H. Wannier, *Phys. Rev.* **52**, 191 (1937).
 - [33] W. Kohn, *Phys. Rev.* **115**, 809 (1959).
 - [34] N. Marzari and D. Vanderbilt, *Phys. Rev. B* **56**, 12847 (1997).